THE JOURNAL OF PHYSICAL CHEMISTRY LETTERS
A JOURNAL OF THE AMERICAN CHEMICAL SOCIETY

pubs.acs.org/JPCL

Letter

Different Mechanisms of DNA Radiosensitization by 8-Bromoadenosine and 2′-Deoxy-2′-fluorocytidine Observed on DNA Origami Nanoframe Supports

Leo Sala, Hlib Lyshchuk, Jana Šáchová, David Chvátil, and Jaroslav Kočišek*

Cite This: *J. Phys. Chem. Lett.* 2022, 13, 3922−3928

Read Online

ACCESS | Metrics & More | Article Recommendations | Supporting Information

ABSTRACT: DNA origami nanoframes with two parallel DNA sequences are used to evaluate the effect of nucleoside substituents on radiation-induced DNA damage. Double strand breaks (DSB) of DNA are counted using atomic force microscopy (AFM), and total number of lesions is evaluated using real-time polymerase chain reaction (RT-PCR). Enhanced AT or GC content does not increase the number of DNA strand breaks. Incorporation of 8-bromoadenosine results in the highest enhancement in total number of lesions; however, the highest enhancement in DSB is observed for 2′-deoxy-2′-fluorocytidine, indicating different mechanisms of radiosensitization by nucleoside analogues with the halogen substituent on base or sugar moieties, respectively. "Bystander" effects are observed, when the number of DSB in a sequence is enhanced by a substituent in the parallel DNA sequence. The present approach eliminates limitations of previously developed methods and motivates detailed studies of poorly understood conformation or bystander effects in radiation induced damage to DNA.

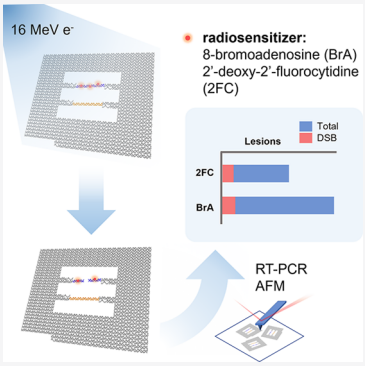

Understanding radiation damage to DNA is crucial for cancer radiotherapy. Irreparable damage to DNA suppresses cell proliferation, thereby exploring its mechanisms is important to the improvement of radio-therapeutic techniques.[1,2] Several tools have been utilized to study radiation damage to DNA in solution, most of them relying on plasmid DNA and gel electrophoresis.[3,4] These can provide quantitative data on DNA damage by ionizing radiation, although they are often influenced by the chosen analysis approach.[5,6] Plasmid DNA-based systems have been useful in fundamental studies, for example, in disentangling direct and indirect effects of radiation on DNA damage[3,7,8] or in studies identifying sources of synergism in chemo-radiation therapy.[9−11] In certain cases, however, plasmid DNA and the necessity for stabilizing buffer solutions create a complex system that could be difficult to link to fundamental studies performed on isolated DNA building blocks.[12,13] Therefore, there is also rising interest in studies of short DNA segments, incorporated into DNA strands[14] or placed in a well-defined environment.[15−17]

DNA origami nanostructures are promising tools to study radiation damage to DNA sequences and radiosensitivity modification by sensitizers such as nucleotides functionalized with electron affinic moieties. The hundreds of synthetic oligomers that compose the origami nanostructure allow for hundreds of unique binding sites that can be extended to support a wide array of probes and active agents at fixed nanometric spaces.[18] A common DNA origami-based technique used to study DNA single strand breaks utilizes DNA origami nanotriangles deposited on Si/SiO_2 substrates with atomic force microscopy (AFM) as the primary characterization technique to quantify strand breaks *in singulo*.[19] Biotinylated DNA oligomers containing sequences of interest are attached to several locations on the origami nanostructure, free-standing above the surface, which can be irradiated in vacuum either by vacuum ultraviolet (VUV) or low energy electrons (LEE). The intact strands remaining after irradiation are amplified by the addition of streptavidin for subsequent visualization by AFM.[19] The technique has been tested on various oligomer sequences with and without added radiosensitizers as well as biologically relevant secondary structures like G-quadruplexes generating values for strand break cross sections to represent the effects of secondary electrons.[20−22] These studies are so far limited to irradiation in vacuum. Extending these studies to systems in aqueous solution as demonstrated in the present study would be beneficial in order to determine the respective contributions of direct effects deduced from said studies and those of indirect effects caused by reactive radiolysis products like OH radicals in environments close to that experienced by DNA in cellular environments. Some exploratory studies on bare origami nanostructures were also performed, indicating another

Received: February 25, 2022
Accepted: April 15, 2022
Published: April 26, 2022

https://doi.org/10.1021/acs.jpclett.2c00584
J. Phys. Chem. Lett. 2022, 13, 3922−3928

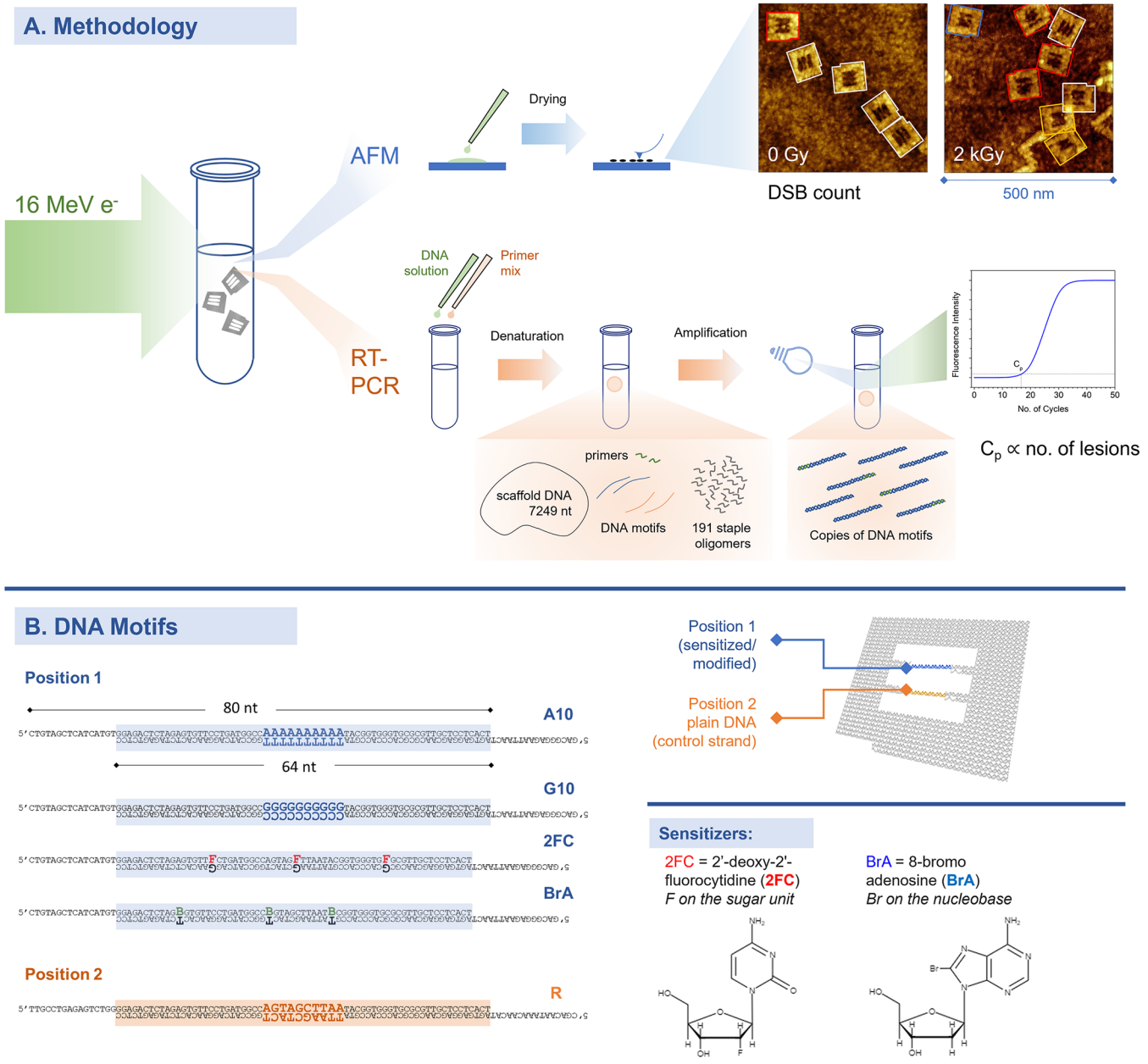

Figure 1. Scheme of the methods employed (A) and the various sequences studied, their positions in the origami nanostructure (image rendered in oxView),[25] and the chemical structures of the radiosensitizers used (B).

possible approach to study DNA damage in the aqueous environment using DNA origami templates. One of these made use of C_{60} in solution to generate $^1O_2$ reactive species upon photoexcitation, which then react with DNA origami[23] as observed through AFM. In another study, solutions containing DNA origami were irradiated by high doses of γ-rays and proton beams, demonstrating enhanced DNA origami stability compared to similarly sized plasmids, making it a suitable substrate for radiation damage studies.[24]

The common use of DNA origami as a substrate with free-standing sequences of interest is limited to sequences of only several nucleotides due to the tendencies of longer sequences (~20 nucleotides) to fold.[26] Here we exploit an alternative method using DNA origami nanoframes, which enables studies of longer double stranded sequences (Figure 1A). The nanoframes are based on the design of the Sugiyama group,[27] where it was mostly used for state of the art mechanistic studies on various DNA sequences.[28,29] The frames are ~80 × 90 nm in dimension and are constructed from an M13mp18 single-stranded DNA scaffold and 222 strategically designed staple oligomer sequences that tie the structure together. We had to trim the blunt ends by the removal of 31 staples on the sides to prevent agglomeration during deposition on the surface as a consequence of $\pi-\pi$ stacking in between the end bases. The frames can support a couple of DNA motifs in their inner aperture, with at least 64 base-pairs in addition to 16 nucleotides that anchor to both sides of the origami frame (Figure 1B). In this design, two duplexes/motifs can be studied at the same time, allowing for direct comparison of damage to the strands, for example, in between two different DNA sequences or in between plain DNA and its sensitized form. We irradiated the samples in solution using 16 MeV electrons, deposited the treated solutions on Si substrates, and then visualized directly the

https://doi.org/10.1021/acs.jpclett.2c00584
J. Phys. Chem. Lett. 2022, 13, 3922−3928

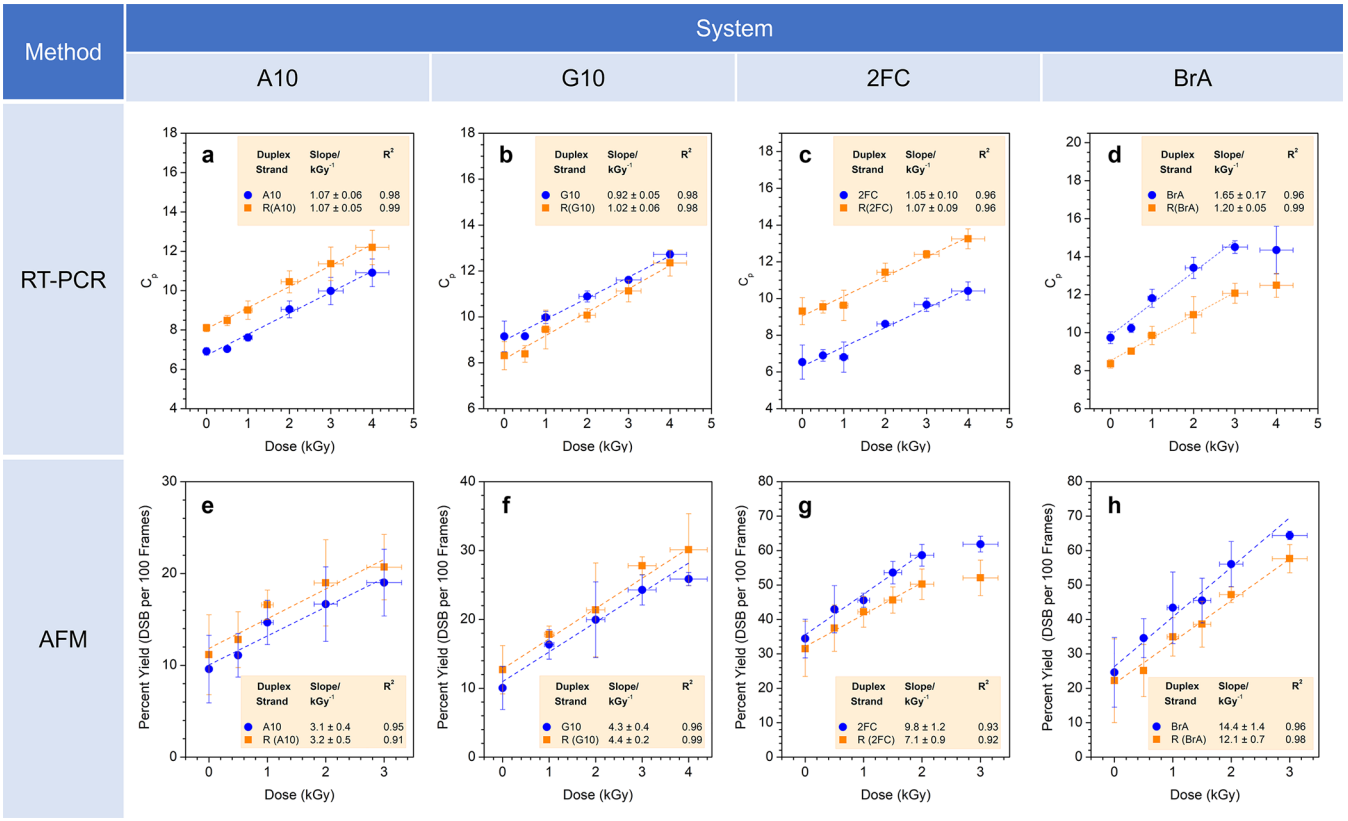

Figure 2. Dose response of C_p values (Mean ± SD, n = 3) from RT-PCR analysis (a–d) and AFM counts of % DSB (Mean ± SD, n = 4–7) vs absorbed dose curves (e–h) of the various DNA motifs studied: A10, G10, 2FC, and BrA (blue circles) and their accompanying control (R) strand (orange squares). Linear fits were performed on each curve based on eqs 3 and 2 for data obtained from RT-PCR and AFM, respectively. Uncertainties in absorbed doses are within 10% as estimated from the measurements of dose rates on the irradiation platform.

strand breaks by AFM. The AFM count is limited to double strand breaks caused both by direct hits as well as double strand breaks from multiple SSBs on both strands of the DNA motif (clustered damages). The rest of the sample was then analyzed using a real-time polymerase chain reaction (RT-PCR), which was used as a complementary analytical technique to confirm dose-dependent damage to the DNA motifs. The latter can detect the relative amount of remaining, intact DNA motifs after irradiation; however, it cannot differentiate between the different types of lesions.

In this work, we investigated four systems, two of which deal with the effects of the AT and GC contents of the strands (referred to here as A10 and G10 systems); the other two concern the effects of the inclusion of model radiosensitizing nucleosides (referred to here as 2FC and BrA systems) (Figure 1B). The A10 system contains a higher AT content with A_{10} and complementary T_{10} fixed within the center of the DNA duplex in the top position (Position 1). The bottom position (Position 2) supports a control strand comprised of a scrambled DNA sequence (R(A10)). In the G10 system, the A_{10}:T_{10} section of the top strand is replaced by a G_{10}:C_{10} sequence. For the radiosensitized systems, the 64 bp free central sequence of the 2FC strand is similar to that of the R strand but with three cytidine nucleosides replaced by 2′-deoxy-2′-fluorocytidine, while in the BrA system, three adenosine nuleosides are replaced by 8-bromoadenosine (Figure 1B). Both are representative models for two types of electrophilic radiosensitizers, with halogen atoms incorporated in the sugar unit[30,31] and the base unit[32,33] of the nucleosides, respectively. In both systems, the R sequence is retained in Position 2 serving as a control.

The breaks in the parallel duplex strands in the frame aperture can be distinguished and counted by AFM. The counts for each system at increasing absorbed dose are shown in Figure 2e–h. The dose response of DSB counted per DNA origami frame (N_{DSB}, with initial DSB count (N_{DSB_0}) in the unirradiated sample) can be described by an exponential with a saturation point (eq 1) and a decay rate corresponding to the double strand break yield (μ_{DSB}) due to the observed stochastic nature of the process.[34] The working range 0–4 kGy (see Supporting Information) before the frames become heavily damaged is still within the quasi-linear regime estimated by fitting a linear function whose slope is equal to μ_{DSB} (eq 2).

$$N_{DSB} = N_{DSB_0} + (1 - e^{-\mu_{DSB}D}) \quad (1)$$

$$N_{DSB} \approx \mu_{DSB}D + N_{DSB_0} \quad (2)$$

In the case of RT-PCR, the fraction of remaining intact strands $\left(\frac{N}{N_0}\right)$ after irradiation is related to the measured C_p (crossing point or threshold value of fluorescence detection) as described in eq 3, taking into account the primer efficiency (E) obtained from standard curves (see Supporting Information), with C_{p,N_0} taken as the threshold value of the control containing N_0 strands.[35,36] The measured curves are shown in Figure 2a–d. During irradiation, the strands can be nicked, and the remaining fraction of intact strands can be related to the absorbed dose (D) by an exponential decay function (eq

https://doi.org/10.1021/acs.jpclett.2c00584
J. Phys. Chem. Lett. 2022, 13, 3922–3928

Table 1. Estimated Strand Break Yields of the Various DNA Motifs Studied after Irradiation with 16 MeV Electrons[a]

DNA Motif	μ_{TL} ± SD (total lesions·kGy^{-1})	EF (total lesions)	μ_{DSB} ± SD (DSB·kGy^{-1})	EF (DSB)
A10	0.73 ± 0.04	1.02 ± 0.07	0.030 ± 0.005	0.98 ± 0.19
R(A10)	0.71 ± 0.03		0.031 ± 0.006	
G10	0.64 ± 0.04	0.95 ± 0.09	0.043 ± 0.004	0.98 ± 0.11
R(G10)	0.67 ± 0.04		0.044 ± 0.002	
2FC	0.70 ± 0.06	0.98 ± 0.12	0.118 ± 0.010	1.27 ± 0.13
R(2FC)	0.71 ± 0.06		0.093 ± 0.005	
BrA	1.19 ± 0.12	1.49 ± 0.16	0.144 ± 0.014	1.19 ± 0.13
R(BrA)	0.79 ± 0.04		0.121 ± 0.007	

[a]The enhancement factors are taken from the ratio of μ_{TL} or μ_{DSB} between the modified strand and the control strand (R) in each system.

Table 2. Strand Break Yields Obtained from This Work and Those Obtained from Gel Electrophoresis Results of High Energy Electron Irradiated Plasmid DNA in the Literature.[a]

plasmid/system	electron energy (MeV)	scavenging capacity (s^{-1})	dose rate (Gy s^{-1})	μ_{SSB} ± SD (SSB·Mbp^{-1}·Gy^{-1})	μ_{DSB} ± SD (DSB·Mbp^{-1}·Gy^{-1})	ref
64 bp duplex on DNA origami frames	16	10^7	6.7	10.58 ± 0.53	0.51 ± 0.10	this work
				9.85 ± 0.7	0.69 ± 0.03	
				9.64 ± 0.95	1.45 ± 0.08	
				10.51 ± 0.57	1.89 ± 0.11	
pBR322	16	7×10^5	0.2	33.25 ± 3.21	0.19 ± 0.07	Perstin et al. 2022[40]
			47	12.22 ± 0.37	0.12 ± 0.04	
			93	13.57 ± 0.57	0.12 ± 0.05	
pBR322	6	10^6	N.S.	7.94 ± 0.14	0.97 ± 0.10	Small et al. 2019[41]
	10			11.00 ± 0.66	1.13 ± 0.08	
	15			7.71 ± 0.03	1.22 ± 0.01	
pBR322	100	10^6	0.5	15.42 ± 0.86	0.35 ± 0.02	Small et al. 2021[42]
	150			17.63 ± 0.57	0.35 ± 0.03	
	200			20.19 ± 0.56	0.38 ± 0.02	
	100	10^6	~10^8 (flash)	20.31 ± 1.20	0.37 ± 0.03	
	150			18.74 ± 0.52	0.37 ± 0.04	
	200			21.22 ± 0.38	0.38 ± 0.02	

[a]The μ_{SSB} values from this work represent the minimum SSB and are estimated from $\mu_{TL} - \mu_{DSB}$ of the R strands in Table 1.

4). The decay rate (μ_{TL}) estimates the number of lesions per absorbed dose assuming a Poisson distribution of nicking events. The lesions include all double strand breaks and all damages to the modified strands that prevent PCR amplification such as single-strand breaks and base damages. Combining both equations relates the RT-PCR raw measurements in terms of C_p and the absorbed dose to directly obtain the number of lesions from the slope of the linear fit of the C_p vs D curves (eq 5).

$$\frac{N}{N_0} = (1 + E)^{(C_{p,N_0} - C_p)} \tag{3}$$

$$\frac{N}{N_0} = e^{-\mu_{TL} D} \tag{4}$$

$$C_p = \frac{\mu_{TL} D}{\ln(1 + E)} - C_{p,N_0} \tag{5}$$

To discuss the effects of GC content, we can first look into the A10 and G10 systems. The values for PCR-evaluated lesions, AFM-evaluated DSB, and the corresponding enhancement factors when comparing the damages to the control strand in Position 2 are summarized in Table 1. Within the sensitivity of the present methods, increasing and decreasing the GC content by incorporation of contiguous G_{10}:C_{10} and A_{10}:T_{10} sequences do not show particular enhancement in the strand break yields. It has been observed that, with low energy electron irradiated sequences in the dry state, oligomers with contiguous guanine and cytosine strands have lesser strand break cross section compared to adenine and thymine;[19] however, certain studies on sequence dependence of γ radiation damage on plasmids in solution, where indirect effects play a significant role, identify cytosine as the preferred damage site for SSB and DSB and guanine for base damage.[37] It appears that both effects play a role in the damage observed for said systems within the radical scavenging conditions of the solution used in this experiment.

For the sensitized strands, in the 2FC system in which the halogen is attached to the sugar unit of the DNA, the total lesions are the same as the control strand as revealed by RT-PCR measurements; however, the double strand break yield is enhanced. So far radiosensitization of 2′-deoxy-2′-fluorocytidine has not yet been explored in the literature, but it appears that it does have a significant effect in increasing DSB damage in irradiated DNA. As the numbers of lesions in the modified and control DNA strands are the same, the mechanism can be explained by the different evolution of clustered damages in the two systems. While clustered DNA damages will remain non-DSB in the random sequence, they will result in DSB in the 2FC enhanced sequence. This can be caused by the formation of sugar radicals known to induce irreversible DNA damages,[38] possibly cutting the neighboring strands or just by the higher susceptibility of the 2FC strand to decay.

https://doi.org/10.1021/acs.jpclett.2c00584
J. Phys. Chem. Lett. 2022, 13, 3922−3928

In the 8-bromoadenosine containing strand, both total lesions and DSB yields are amplified compared to the nonsensitized strand. The enhancement on DSB is lower than that on total lesions, which means that the strand breaks on the brominated base do not mostly result in DSB. The DNA sensitization by 8-bromoadenosine was explored in experiments with low-energy electrons irradiating single-stranded DNA sequences immobilized on DNA origami nanotriangles[39] and explained by experiments with isolated molecules.[33] An average enhancement factor of 1.9 ± 0.6 for irradiations by electrons in the 0.5−9 eV range was observed when comparing 8-bromoadenosine incorporated strands with the same sequence without the sensitizer, not far from the enhancement observed here for total lesions.

The damage profiles for 2FC and BrA indicate that the mechanisms of sensitization by these compounds are different. While BrA enhances number of single strand breaks, 2FC amplifies the number of DSB damages at the same SSB level.

It can be noted that the number of DSBs on the R strand in Position 2 is also increased by the presence of sensitized strands (R(2FC) and R(BrA) in Table 1)) when compared to the R strand in the presence of A/G enhanced strands (R(A10) and (R(G10) in Table 1). This can be explained as "bystander" effects, when release and diffusion of reactive species from the fragmentation of the sensitized strand can cause damages in the neighboring random sequence. In the present nanoframe design, the distance between the parallel strands is ∼12 nm. However, the DNA origami technique allows for change of the distance by redesigning the nanoframe and can thus elicit more detailed exploration of this effect not only with respect to different sequences of DNA strands but also the incorporation of various types of radiosensitizers such as gold nanoparticles, which we plan to explore in the future.

Lastly, we can also compare the results of the strand break yields obtained from RT-PCR and AFM to that observed in plasmid irradiated studies at similar conditions. While DSBs can be directly compared, the number of lesions do not exactly correspond to the number of single-strand breaks. As described earlier, these encompass strand breaks and base damages on the PCR amplified strand of the double stranded DNA sequence, and therefore, the given numbers are only the lowest estimates of the SSBs. The estimates for the control strands are shown in Table 2 and are within the range of strand break yields observed in the literature. It is difficult to directly compare the values due to the differences in parameters such as the radical scavenging capacities and dose rates utilized, but both absolute values and SSB to DSB ratios are within the same range. We therefore believe that the present method can be a viable substitute or complementary technique to assess radiation induced damage to DNA sequences in solution. The nanoframe approach also allows new questions to be addressed in radiation damage such as evaluating "bystander" effects with nanometer precision as well as consequences of such damage to DNA conformation.

To conclude, we demonstrated the use of DNA origami frames to study radiation damage to doubly stranded DNA sequences in aqueous solution, particularly in assessing double strand breaks and radiosensitization/enhancement factors of halogenated nucleosides by AFM. RT-PCR was used to confirm dose-dependent damage by detecting the relative amount of remaining intact DNA motifs. The introduction of contiguous sequences of A-T and G-C base pairs did not result in changes in strand break yields detectable by the present approach. Introducing fluorine on the sugar unit of the DNA does not significantly induce more lesions compared to the unsensitized DNA strand but has enhanced double strand break yields. Bromoadenine consistently shows strand break enhancement both for total lesion and for double strand breaks. The strand break yields obtained using the method are close to those obtained in plasmid irradiated with MeV electrons; hence, it can be a promising tool to study radiation damage to DNA sequences of interest.

■ ASSOCIATED CONTENT

Supporting Information

The Supporting Information is available free of charge at https://pubs.acs.org/doi/10.1021/acs.jpclett.2c00584.

Methods, radiation damage to DNA origami nanoframes, and DNA origami staple sequences (PDF)

Transparent Peer Review report available (PDF)

■ AUTHOR INFORMATION

Corresponding Author

Jaroslav Kočišek − *J. Heyrovský Institute of Physical Chemistry of CAS, 18223 Prague, Czech Republic;* orcid.org/0000-0002-6071-2144; Email: jaroslav.kocisek@jh-inst.cas.cz

Authors

Leo Sala − *J. Heyrovský Institute of Physical Chemistry of CAS, 18223 Prague, Czech Republic;* orcid.org/0000-0003-1091-4386

Hlib Lyshchuk − *J. Heyrovský Institute of Physical Chemistry of CAS, 18223 Prague, Czech Republic;* orcid.org/0000-0003-3964-4164

Jana Šáchová − *Laboratory of Genomics and Bioinformatics, Institute of Molecular Genetics of the CAS, 142 20 Prague, Czech Republic*

David Chvátil − *Nuclear Physics Institute of the CAS, 250 68 Řež, Czech Republic*

Complete contact information is available at: https://pubs.acs.org/10.1021/acs.jpclett.2c00584

Notes

The authors declare no competing financial interest.

■ ACKNOWLEDGMENTS

This work was supported by the Czech Science Foundation, Project No. 21-26601X, and projects "Center for Tumor Ecology - Research of the Cancer Microenvironment Supporting Cancer Growth and Spread" (Reg. No. CZ.02.1.01/0.0/0.0/16_019/0000785) and CARAT "Carbon allotropes with rationalized nanointerfaces and nanolinks for environmental and biomedical applications" (Reg. No. CZ.02.1.01/0.0/0.0/16_026/0008382) supported by the Operational Programme Research, Development and Education.

■ REFERENCES

(1) Huang, R.-X.; Zhou, P.-K. DNA Damage Response Signaling Pathways and Targets for Radiotherapy Sensitization in Cancer. *Signal Transduct. Target. Ther.* **2020**, *5*, 60.

(2) Seiwert, T. Y.; Salama, J. K.; Vokes, E. E. The Concurrent Chemoradiation Paradigm—General Principles. *Nat. Clin. Pract. Oncol.* **2007**, *4*, 86−100.

(3) Alizadeh, E.; Orlando, T. M.; Sanche, L. Biomolecular Damage Induced by Ionizing Radiation: The Direct and Indirect Effects of Low-Energy Electrons on DNA. *Annu. Rev. Phys. Chem.* **2015**, *66*, 379−398.
(4) Huwaidi, A.; Kumari, B.; Robert, G.; Guérin, B.; Sanche, L.; Wagner, J. R. Profiling DNA Damage Induced by the Irradiation of DNA with Gold Nanoparticles. *J. Phys. Chem. Lett.* **2021**, *12*, 9947−9954.
(5) Śmiałek, M. A.; Moore, S. A.; Mason, N. J.; Shuker, D. E. G. Quantification of Radiation-Induced Single-Strand Breaks in Plasmid DNA using a TUNEL/ELISA-Based Assay. *Radiat. Res.* **2009**, *172*, 529−536.
(6) Pachnerová Brabcová, K.; Sihver, L.; Ukraintsev, E.; Štěpán, V.; Davídková, M. How Detection of Plasmid DNA Fragmentation Affects Radiation Strand Break Yields. *Radiat. Prot. Dosim.* **2019**, *183*, 89−92.
(7) Gao, Y.; Zheng, Y.; Sanche, L. Low-Energy Electron Damage to Condensed-Phase DNA and Its Constituents. *Int. J. Mol. Sci.* **2021**, *22*, 7879.
(8) Dong, Y.; Gao, Y.; Liu, W.; Gao, T.; Zheng, Y.; Sanche, L. Clustered DNA Damage Induced by 2−20 eV Electrons and Transient Anions: General Mechanism and Correlation to Cell Death. *J. Phys. Chem. Lett.* **2019**, *10*, 2985−2990.
(9) Schlatholter; Lacombe, S.; Eustache, P.; Porcel, E.; Salado, D.; Stefancikova, L.; Tillement, O.; Lux, F.; Mowat, P.; van Goethem, M.-J.; Remita, H.; Biegun, A.; et al. Improving proton therapy by metal-containing nanoparticles: nanoscale insights. *Int. J. Nanomedicine* **2016**, *11*, 1549−1556.
(10) Rezaee, M.; Sanche, L.; Hunting, D. J. Cisplatin Enhances the Formation of DNA Single- and Double-Strand Breaks by Hydrated Electrons and Hydroxyl Radicals. *Radiat. Res.* **2013**, *179*, 323−331.
(11) Reimitz, D.; Davídková, M.; Mestek, O.; Pinkas, J.; Kočišek, J. Radiomodifying effects of RAPTA C and CDDP on DNA strand break induction. *Radiat. Phys. Chem.* **2017**, *141*, 229−234.
(12) Hahn, M. B.; Meyer, S.; Schröter, M.-A.; Seitz, H.; Kunte, H.-J.; Solomun, T.; Sturm, H. Direct Electron Irradiation of DNA in a Fully Aqueous Environment. Damage Determination in Combination with Monte Carlo Simulations. *Phys. Chem. Chem. Phys.* **2017**, *19*, 1798−1805.
(13) Ribar, A.; Huber, S. E.; Śmiałek, M. A.; Tanzer, K.; Neustetter, M.; Schürmann, R.; Bald, I.; Denifl, S. Hydroperoxyl Radical and Formic Acid Formation from Common DNA Stabilizers upon Low Energy Electron Attachment. *Phys. Chem. Chem. Phys.* **2018**, *20*, 5578−5585.
(14) Balasubramanian, B.; Pogozelski, W. K.; Tullius, T. D. DNA Strand Breaking by the Hydroxyl Radical is Governed by the Accessible Surface Areas of the Hydrogen Atoms of the DNA Backbone. *Proc. Natl. Acad. Sci. U. S. A.* **1998**, *95*, 9738−9743.
(15) Solomun, T.; Hultschig, C.; Illenberger, E. Microarray Technology for the Study of DNA Damage by Low-Energy Electrons. *Eur. Phys. J. D* **2005**, *35*, 437−441.
(16) Schürmann, R.; Vogel, S.; Ebel, K.; Bald, I. The Physico-Chemical Basis of DNA Radiosensitization: Implications for Cancer Radiation Therapy. *Chem. Eur. J.* **2018**, *24*, 10271−10279.
(17) Li, Z.; Cloutier, P.; Sanche, L.; Wagner, J. R. Low-Energy Electron-Induced DNA Damage: Effect of Base Sequence in Oligonucleotide Trimers. *J. Am. Chem. Soc.* **2010**, *132*, 5422−5427.
(18) Dey, S.; Fan, C.; Gothelf, K. V.; Li, J.; Lin, C.; Liu, L.; Liu, N.; Nijenhuis, M. A. D.; Saccà, B.; Simmel, F. C.; et al. DNA Origami. *Nat. Rev. Methods Primers* **2021**, *1*, 13.
(19) Vogel, S.; Rackwitz, J.; Schürman, R.; Prinz, J.; Milosavljević, A. R.; Réfrégiers, M.; Giuliani, A.; Bald, I. Using DNA Origami Nanostructures To Determine Absolute Cross Sections for UV Photon-Induced DNA Strand Breakage. *J. Phys. Chem. Lett.* **2015**, *6*, 4589−4593.
(20) Rackwitz, J.; Bald, I. Low-Energy Electron-Induced Strand Breaks in Telomere-Derived DNA Sequences—Influence of DNA Sequence and Topology. *Chem. Eur. J.* **2018**, *24*, 4680−4688.
(21) Keller, A.; Bald, I.; Rotaru, A.; Cauët, E.; Gothelf, K. V.; Besenbacher, F. Probing Electron-Induced Bond Cleavage at the Single-Molecule Level Using DNA Origami Templates. *ACS Nano* **2012**, *6*, 4392−4399.
(22) Keller, A.; Rackwitz, J.; Cauët, E.; Liévin, J.; Körzdörfer, T.; Rotaru, A.; Gothelf, K. V.; Besenbacher, F.; Bald, I. Sequence Dependence of Electron-induced DNA Strand Breakage Revealed by DNA Nanoarrays. *Sci. Rep.* **2015**, *4*, 7391.
(23) Ray, A.; Liosi, K.; Ramakrishna, S. N.; Spencer, N. D.; Kuzuya, A.; Yamakoshi, Y. Single-Molecule AFM Study of DNA Damage by $^1O_2$ Generated from Photoexcited C60. *J. Phys. Chem. Lett.* **2020**, *11*, 7819−7826.
(24) Sala, L.; Zerolová, A.; Rodriguez, A.; Reimitz, D.; Davídková, M.; Ebel, K.; Bald, I.; Kočišek, J. Folding DNA into Origami Nanostructures Enhances Resistance to Ionizing Radiation. *Nanoscale* **2021**, *13*, 11197−11203.
(25) Poppleton, E.; Bohlin, J.; Matthies, M.; Sharma, S.; Zhang, F.; Šulc, P. Design, optimization and analysis of large DNA and RNA nanostructures through interactive visualization, editing and molecular simulation. *Nucleic Acids Res.* **2020**, *48*, e72.
(26) Ebel, K.; Bald, I. Length and Energy Dependence of Low-Energy Electron-Induced Strand Breaks in Poly(A) DNA. *Int. J. Mol. Sci.* **2020**, *21*, 111.
(27) Endo, M.; Katsuda, Y.; Hidaka, K.; Sugiyama, H. Regulation of DNA Methylation Using Different Tensions of Double Strands Constructed in a Defined DNA Nanostructure. *J. Am. Chem. Soc.* **2010**, *132*, 1592−1597.
(28) Endo, M.; Katsuda, Y.; Hidaka, K.; Sugiyama, H. A Versatile DNA Nanochip for Direct Analysis of DNA Base-Excision Repair. *Angew. Chem., Int. Ed.* **2010**, *49*, 9412−9416.
(29) Sannohe, Y.; Endo, M.; Katsuda, Y.; Hidaka, K.; Sugiyama, H. Visualization of Dynamic Conformational Switching of the G-Quadruplex in a DNA Nanostructure. *J. Am. Chem. Soc.* **2010**, *132*, 16311−16313.
(30) Adhikary, A.; Kumar, A.; Rayala, R.; Hindi, R. M.; Adhikary, A.; Wnuk, S. F.; Sevilla, M. D. One-Electron Oxidation of Gemcitabine and Analogs: Mechanism of Formation of C3′ and C2′ Sugar Radicals. *J. Am. Chem. Soc.* **2014**, *136*, 15646−15653.
(31) Kopyra, J.; Keller, A.; Bald, I. On the Role of Fluoro-Substituted Nucleosides in DNA Radiosensitization for Tumor Radiation Therapy. *RSC Adv.* **2014**, *4*, 6825−6829.
(32) Wityk, P.; Wieczór, M.; Makurat, S.; Chomicz-Mańka, L.; Czub, J.; Rak, J. Dominant Pathways of Adenosyl Radical-Induced DNA Damage Revealed by QM/MM Metadynamics. *J. Chem. Theory Comput.* **2017**, *13*, 6415−6423.
(33) Schürmann, R.; Tanzer, K.; Dabkowska, I.; Denifl, S.; Bald, I. Stability of the Parent Anion of the Potential Radiosensitizer 8-Bromoadenine Formed by Low-Energy (< 3 eV) Electron Attachment. *J. Phys. Chem. B* **2017**, *121*, 5730−5734.
(34) González, L. N.; Arruda-Neto, J. D. T.; Cotta, M. A.; Carrer, H.; Garcia, F.; Silva, R. A. S.; Moreau, A. L. D.; Righi, H.; Genofre, G. C. DNA fragmentation by gamma radiation and electron beams using atomic force microscopy. *J. Biol. Phys.* **2012**, *38*, 531−542.
(35) Lim, S.; Yoon, H.; Ryu, S.; Jung, J.; Lee, M.; Kim, D. A Comparative Evaluation of Radiation-Induced DNA Damage using Real-Time PCR: Influence of Base Composition. *Radiat. Res.* **2006**, *165*, 430−437.
(36) Svec, D.; Tichopad, A.; Novosadova, V.; Pfaffl, M. W.; Kubista, M. How Good is a PCR Efficiency Estimate: Recommendations for Precise and Robust qPCR Efficiency Assessments. *Biomol. Detect. Quantif.* **2015**, *3*, 9−16.
(37) Murray, V.; Hardie, M. E.; Gautam, S. D. Comparison of Different Methods to Determine the DNA Sequence Preference of Ionising Radiation-Induced DNA Damage. *Genes* **2020**, *11*, 8.
(38) Chatgilialoglu, C. *Radical and Radical Ion Reactivity in Nucleic Acid Chemistry*; John Wiley & Sons, Ltd.: 2009; Chapter 4, pp 99−133.
(39) Schürmann, R.; Tsering, T.; Tanzer, K.; Denifl, S.; Kumar, S. V. K.; Bald, I. Resonant Formation of Strand Breaks in Sensitized

https://doi.org/10.1021/acs.jpclett.2c00584
J. Phys. Chem. Lett. 2022, 13, 3922−3928

Oligonucleotides Induced by Low-Energy Electrons (0.5−9 eV). *Angew. Chem., Int. Ed.* **2017**, *56*, 10952−10955.
(40) Perstin, A.; Poirier, Y.; Sawant, A.; Tambasco, M. Quantifying the DNA-Damaging Effects of FLASH Irradiation with Plasmid DNA. *Int. J. Radiat. Oncol. Biol. Phys.* **2022**, DOI: 10.1016/j.ijrobp.2022.01.049.
(41) Small, K.; Angal-Kalinin, D.; Chadwick, A.; Edge, R.; Henthorn, N.; Jones, R.; Kirkby, K.; Merchant, M.; Morris, R.; Santina, E.; et al. A Comparative Study of Biological Effects of Electrons and Co-60 Gamma Rays on pBR322 Plasmid DNA. *Proc. of the 10th Int. Particle Accelerator Conf.* **2019**, 3533−3536.
(42) Small, K. L.; Henthorn, N. T.; Angal-Kalinin, D.; Chadwick, A. L.; Santina, E.; Aitkenhead, A.; Kirkby, K. J.; Smith, R. J.; Surman, M.; Jones, J.; et al. Evaluating Very High Energy Electron RBE from nanodosimetric pBR322 plasmid DNA damage. *Sci. Rep.* **2021**, *11*, 3341.

https://doi.org/10.1021/acs.jpclett.2c00584
J. Phys. Chem. Lett. 2022, 13, 3922−3928